

## Systematic Identification of Synergistic Drug Pairs Targeting HIV

Xu Tan<sup>1</sup>, Long Hu<sup>2,#</sup>, Lovelace J. Luquette III<sup>3,#</sup>, Geng Gao<sup>1</sup>, Yifang Liu<sup>2</sup>, Hongjing Qu<sup>1</sup>, Ruibin Xi<sup>3</sup>, Zhi John Lu<sup>2,\*</sup>, Peter J. Park<sup>3,\*</sup>, and Stephen J. Elledge<sup>1</sup>

<sup>1</sup>Howard Hughes Medical Institute, Department of Genetics, Harvard Medical School, Division of Genetics, Brigham and Women's Hospital, Boston, MA 02115, USA

<sup>2</sup>MOE Key Laboratory of Bioinformatics, School of Life Sciences, Tsinghua University, Beijing 100084, China

<sup>3</sup>Center for Biomedical Informatics, Harvard Medical School, Boston, MA 02115, USA

### Abstract

The systematic identification of effective drug combinations has been hindered by the unavailability of methods that can explore the large combinatorial search space of drug interactions. Here we present a multiplex screening method named *MuSIC* (Multiplex Screening for Interacting Compounds), which expedites the comprehensive assessment of pair-wise compound interactions. We examined ~500,000 drug pairs from 1000 FDA-approved or clinically tested drugs and identified drugs that synergize to inhibit HIV replication. Our analysis reveals an enrichment of anti-inflammatory drugs in drug combinations that synergize against HIV, indicating HIV benefits from inflammation that accompanies its infection. Multiple drug pairs identified in this study, including glucocorticoid and nitazoxanide, synergize by targeting different steps of the HIV life cycle. As inflammation accompanies HIV infection, our findings indicate that inhibiting inflammation could curb HIV propagation. *MuSIC* can be applied to a wide variety of disease-relevant screens to facilitate efficient identification of compound combinations.

### Keywords

Combination therapy; FDA-approved drug library; HIV

### Introduction

HIV has plagued humans for 30 years, infecting 60 million people and causing over 25 million deaths. AIDS patients can be effectively treated with Highly Active Antiretroviral Therapy (HAART), which usually comprises a combination of three anti-HIV drugs<sup>1</sup>.

---

Users may view, print, copy, download and text and data- mine the content in such documents, for the purposes of academic research, subject always to the full Conditions of use: [http://www.nature.com/authors/editorial\\_policies/license.html#terms](http://www.nature.com/authors/editorial_policies/license.html#terms)

Correspondence should be addressed to S.J.E (selledge@genetics.med.harvard.edu)..

<sup>#</sup>These authors contributed equally to the work.

<sup>\*</sup>These authors contributed equally to the work.

**Conflict of interest statement** The authors declare no competing financial interests.

**Contributions** X.T. & S.E. designed the experiments, X.T., G.G., H.Q. conducted experiments, L.J.L., R.X. & P.J.P developed the algorithm of library construction, L.H., Y.L. & Z.J.L. performed bioinformatic analysis. All authors contributed to manuscript writing.

However, the cost of current HAART therapy is prohibitive in developing countries. In addition, long-term HAART therapy can have serious side effects such as lipodystrophy, hyperglycemia, pancreatitis and liver toxicity<sup>2</sup>. New therapies are needed to expand the current HAART repertoire, to provide hope for a cure and to reduce the cost of treatment and side-effects<sup>3,4</sup>.

Combination therapies are also widely used to treat other infections including hepatitis C virus, malaria and bacterial infections such as pneumonia, in addition to non-infectious diseases such as cancer and asthma<sup>5</sup>. Major benefits of combination therapy include a substantially reduced chance of evolving drug resistance, improved efficacy and reduced side-effects<sup>6</sup>. The large combinatorial space of existing drugs provides a largely untapped resource for developing new treatments. Exploiting this resource could accelerate the drug development process since drugs in current or past use have favorable pharmacological properties. However, the large number of possible combinations from even a modest number of drugs makes a systematic search difficult without an efficient method. For example, for 10 drugs, there are 45 pair-wise combinations; for 100 drugs, 4950; and for 1000 drugs, 499,500.

Systematic searches for synergistic drug combinations have been performed previously in industrial settings using exhaustive combinations<sup>7,8</sup>, but the high cost of this method prevents wide adoption. Pooled screening methods have been explored to identify enzyme inhibitors<sup>9</sup> and to look for synergistic anti-inflammatory compound pairs<sup>10</sup> although the latter study did not yield novel synergistic compound pairs. Here we develop a pooled screening method named *MuSIC* (*Multiplex Screen for Interacting Compounds*) to screen a large collection of diverse FDA-approved or clinically-tested compounds. The *MuSIC* screening library was designed to contain 10 compounds in each well of a 384-well plate and cover all the possible pair-wise combinations among these compounds using less than 3% of the number of wells needed in a standard pair-wise screen. For pools that contain potentially synergistic interactions, we deconvolute each pool into 45 drug pairs to identify efficacious drug pairs. Subsequently, we perform dose titration of the drug pairs to verify whether drugs act in synergy (Fig. 1A). We validate our method using cell-based models of the HIV life cycle and show that it is effective at identifying pair-wise combinations that have anti-HIV activity.

## Results

### Design, Construction and Screening of the MuSIC library

We assembled 1000 compounds from two commercially available drug libraries and the NIH Clinical Collection of compounds that have been tested clinically (Table S1). We performed a preliminary drug screen on our cell line to eliminate potentially toxic chemicals. We also eliminated compounds that are: 1) mainly used topically; 2) cytotoxic compounds; 3) redundant compounds that are structurally related to compounds already selected; 4) existing HAART compounds and other antivirals that might dominate a pool. We aimed to use a minimal number of wells to efficiently assess all the possible pairs among the 1000 compounds. We chose the pool size of 10 due to the tradeoff between the number of pools required and the amount of deconvolution. Since it is not possible to

construct pools of 10 drugs such that every pair in the 1,000-compound library occurs in exactly one pool, we developed a heuristic which guarantees that each drug pair occurs in at least one pool and aims to minimize the number of redundant pairs (Fig. 1A and Supplementary Fig. S1). This heuristic produced 13,106 pools, which is 2.6% of the number of wells needed for testing all pairwise interactions separately and only 18% larger than the theoretical lower bound of 11,100 pools. The arrayed library consists of forty-five 384-well plates in which each compound is present at a concentration of 0.1–0.2 mg/ml in DMSO (Supplementary Fig. S2).

We used HeLa-based MAGI cells that express the CD4 receptor<sup>11</sup>, and the IIB strain of HIV for our screening assay. Our screen utilizes a two-part assay modified from our previously reported siRNA screen (Fig. 1B)<sup>12</sup>. The part one assay consists of incubating cells for 18 h with drugs followed by viral infection. After 48 h, HIV infectivity is measured by detection of the HIV p24 antigen using immunostaining and automated fluorescence imaging. Nuclear staining and imaging are also carried out on the same plates to assess cell proliferation and cytotoxicity of the drugs. The part one assay measures the viral infection steps from entry to protein translation.

In the part two assay the supernatant from part one is transferred to fresh cells and, 48 h later, those cells are stained for p24 and nuclei. This quantifies the number of new viral particles produced in the part one assay and both reinforces the results of the part one assay and complements it by detecting later stages of the HIV life cycle including viral assembly, budding and infectivity. This two-part screening strategy was optimized using the known anti-HIV drugs AZT and nevirapine as positive controls and DMSO as the negative control (Fig. 1C and Supplementary Fig. S3).

### **MuSIC screening identifies synergistic anti-HIV drug pairs**

From the primary screen of the pooled library using the two-part assay performed in triplicate (Supplementary Table S2), we selected 288 pools for deconvolution based on their low infection rate and low cytotoxicity, resulting in 12,904 unique drug pairs. We constructed a secondary library to deconvolute the 288 pools and identify potent drug pairs. We used another heuristic to design the layout of the plates of the secondary library to account for the high variability in drug representation in the secondary library and the limit on available drug volume (Supplementary Fig. S2). This secondary library was screened in triplicate using the same two-part assay (secondary screen) (Supplementary Table S3). We validated the results of the secondary screen by selecting the top 116 pairs that reduced the infection rate of either the part one or the part two assay by at least 50% and carrying out concentration titration experiments. Of the 116 pairs, 104 (90%) reduced HIV infection rate by 50% in the part two assay in at least one concentration combination used in the titration. (Supplementary Table S4).

To measure synergy between drugs, we used two popular models, Bliss independence and Higher Single Activity (HSA)<sup>7</sup>. The Bliss model is based on probability theory and assumes that when two drugs are independent, their combinatorial effect should be the multiplication of their individual effects. The HSA model defines synergy as a combinatorial effect that is larger than any of the individual drug's effects at the same concentrations as present in the

mixture. To increase the stringency of our criteria, we require that at least three dose combinations produce a 10% reduction of normalized HIV infection over that predicted by the synergy models. According to the Bliss model, 66 of the 116 pairs (57%) showed synergy using these criteria. For the HSA model, 77 pairs (66%) are synergistic. 41 pairs (35%) are synergistic using both models (Supplementary Table S5). Notably, a top pool (producing among the largest reduction in HIV infection rates) identified in the primary screen (Fig. 2A) produced a top-ranked pair in the secondary screen, comprising the glucocorticoid drug betamethasone and an anti-protozoal drug nitazoxanide (Fig. 2B, C), indicating the effectiveness of this primary and secondary screening strategy. We also observed that multiple drugs in the top pairs from the part one screen belong to a small set of functional groups including glucocorticoids, non-steroidal anti-inflammatory drugs (NSAIDs) and anti-cholinergic drugs (Fig. 4A, also discussed below). The four glucocorticoids present in our library appeared most frequently among the top pairs.

### A separate screen validates the MuSIC strategy

To systematically validate the MuSIC method, we performed a separate screen to directly look for drugs that synergize with the glucocorticoid prednisolone (PDN) since glucocorticoids were highly represented in the top pairs. This screen was done using the part one assay with each well containing PDN and one of the 1000 drugs in the MuSIC library. We found that nitazoxanide consistently displays the highest synergy with PDN (Fig. 2C). In addition, among the top 15 hits from this direct screen (Z score < -1.5) seven were also scored as hits in the MuSIC screen (Z score < -1.5), a discovery rate of 46.7% (p value <  $10^{-13}$ , binomial test) (Supplementary Tables S3 and S6). These findings clearly demonstrate that the *MuSIC* strategy can effectively identify strongly synergistic drug pairs.

### Validation of the synergy of glucocorticoid and nitazoxanide

Glucocorticoids are widely used anti-inflammatory drugs and their inhibition of HIV has been primarily attributed to reduction of HIV-LTR driven transcription<sup>13, 14</sup>. In clinical trials glucocorticoid has been shown to be protective against CD4+ T cell loss due to HIV infection<sup>15, 16</sup>. Nitazoxanide (NTZ) was approved for treating cryptosporidiosis in 2004 and later found to have activities against the hepatitis C<sup>17</sup>, hepatitis B<sup>17</sup> and influenza A viruses<sup>18</sup> in cellular assays but its anti-HIV activity has not been previously reported. The synergy between these two drugs was confirmed by two distinct methods to quantify drug synergy: the Bliss independence model<sup>19</sup> and the Combination Index method based on the additivity model (CI)<sup>20</sup>. By contrast, the Loewe additivity model assumes that the combination should have the same effect as one of the single agents, but at a higher concentration corresponding to the addition of equally effective doses<sup>6</sup>. The combinatorial effects of glucocorticoid and NTZ are substantially larger at multiple doses than those predicted by the Bliss model (Fig. 2D). Combination Indices calculated at three activity levels and two dose ratios all indicate strong (CI < 0.3) or very strong synergy (CI < 0.1) between the glucocorticoid prednisolone (PDN) and NTZ (Fig. 2G). This synergy is achieved with no cytotoxicity as measured by cell proliferation in the three-day assay. We confirmed the synergy between glucocorticoid and NTZ in a T-cell line (Jurkat cells) using a reporter assay (Supplementary Fig. S7). We also tested the anti-HIV effect of PDN and nitazoxanide (TIZ, the metabolic product and active form of NTZ) in primary peripheral blood

mononuclear cells (PBMCs). In the PBMC assay, p24 ELISA was used to quantify HIV replication seven days post infection. The synergy of PDN and TIZ in anti-viral activity is very significant, for example, 2  $\mu$ M TIZ reduces infection by 10%, 2  $\mu$ M PDN has a 51% reduction, but combined, they reduce infection by 79% (Fig. 2H). The toxicity in this stringent seven-day assay due to PDN is mild, for example, at 10  $\mu$ M, the reduction of viability measured by CellTiter Glo assay is about 27%. Importantly, there is no additional toxicity caused by combining TIZ with PDN (Supplementary Fig. S8).

### Glucocorticoid and Nitazoxanide target different steps of the HIV life cycle

We next tested combinations of PDN or NTZ with known anti-HIV drugs for synergy. Interestingly, while both PDN and NTZ synergize with the HIV integrase inhibitor raltegravir (RAL) (Fig. 3C & 3D), only PDN synergizes with the nucleoside reverse transcriptase inhibitor AZT (Fig. 3B). NTZ displays an exact Bliss independence in combination with AZT (Fig. 3A). Similar patterns were observed with the non-nucleoside reverse transcriptase inhibitor efavirenz (EFV) (Fig. 3E & 3F) and no synergy was detected between AZT and efavirenz (Fig. 3G). We also performed Combination Index analysis of the data (Supplementary Fig. S9). This model seems to be more lenient than the Bliss model for judging synergy as all of the analyzed pairs have  $CI_{50}$  (Combination index at 50% efficacy level) below 1, indicating synergy. Nevertheless, we consistently observe that the  $CI_{50}$  of NTZ in combinations with other drugs is very similar to those of reverse transcription inhibitors (AZT or EFV) in combination with the same drugs, while PDN has a significantly lower  $CI_{50}$ . We suspect the similarity of synergy patterns of NTZ and reverse transcription inhibitors might be due to their overlapping mechanisms of actions, as a previous study found a correlation between drug interaction profiles and their mechanism of action<sup>21</sup>. To test this hypothesis, we infected MAGI cells using vesicular stomatitis virus envelope glycoprotein (VSV-g) pseudo-typed HIV NL4-3 virus and measured the product of HIV reverse transcription (late-RT) and its derivative (2-LTR circles) by quantitative real time PCR. NTZ significantly inhibited reverse transcription while PDN had no effect (Fig. 3H). The same experiment was carried out using the T cell line SupT1 and similar results were obtained (Supplementary Fig. S10). We also used a BlaM assay to measure viral entry<sup>22</sup> and found that NTZ does not affect the entry step (Supplementary Fig. S11), therefore NTZ works after viral entry but before, or at, reverse transcription. By contrast, glucocorticoid inhibits a step later than reverse transcription, consistent with prior studies that showed that glucocorticoid reduces HIV LTR-driven transcription<sup>13,14</sup>. No inhibition of reverse transcription by NTZ was observed using an *in vitro* reverse transcription enzymatic assay (Supplementary Fig. S12), indicating that any inhibition is indirect. We conclude that synergy between NTZ and glucocorticoid likely results from targeting different steps in the HIV life cycle.

### Systematic analysis of synergistic drugs pairs

The *MuSIC* screen examined almost half a million drug pairs. To extract drug-drug interaction information from this screen, we performed a computational analysis of the result of the secondary screen of drug pairs. We took advantage of the fact that each drug is present in multiple pairs in the secondary library to derive an average effect for each drug and to estimate the synergy, additivity or antagonism between drugs. Adapting a previously

developed scoring method<sup>23</sup>, we derived a drug-drug interaction network in terms of anti-HIV activity and synergy between drugs. Fig. 4 shows the extracted networks of drugs that ranked tops in terms of anti-viral activity and degree of synergy with other drugs in the part one and two assays (see supplementary text for the scoring method and drug selection criteria), which indicates significant anti-HIV activity both in combination and alone. We constructed two networks, one for drugs that score in the part one assay, and one for those that score only in the part two assay. Drug pairs in the “part one” network significantly reduce infection rates in both part one and part two assays, indicating their effects early in the assay. For the “part two only” network, we required the pairs to have a strong anti-viral activity in the part two assay but not in the part one assay, thus reflecting their functions at the later stages of the viral life cycle. We also required the selected drugs to have more than one potent synergistic interaction with other drugs, which simplified the network depiction and increased the confidence of the network shown. The part one network enriched for drugs with previously demonstrated anti-HIV activity (p-value <  $10^{-12}$ ,  $\chi^2$  test)(Fig. 4, Supplementary Table S7). In addition, functional annotation analysis shows that several drug classes have multiple drugs represented including glucocorticoids, NSAIDs, muscarinic cholinergic receptor antagonists and quinolone. Another feature of this network is the enrichment for drugs that have anti-inflammatory properties (p-value <  $10^{-4}$ ,  $\chi^2$  test). The two widely used anti-inflammatory drug categories are highly enriched with 4 glucocorticoids and 5 NSAIDs. Other drugs in the network with known anti-inflammatory functions include ascorbic acid, rapamycin, a statin drug, a PDE4 inhibitor-rolipram and a  $\beta$ -adrenoreceptor agonist (Supplementary Table S8). By contrast, the “part two only” network comprises very different drug groups. Only one drug in this network has previously been shown to have anti-HIV activity, probably because previous drug screens primarily examined the early steps of viral infection. This part two assay identified novel targets for HIV therapies that inhibit viral assembly and release. The different targets of the drugs in the part one and two networks suggest that there may be synergy between these two groups, which is indeed the case (Fig. 4 green links between the two networks).

## Discussion

We report the development of a drug screening method to identify drug-drug interactions among 1000 FDA-approved or clinically tested drugs that collectively represent a significant portion of the chemical space of current clinical use. We demonstrate this method is effective at selecting drug pairs with strong efficacy and synergy as validated by concentration titration experiments and an independent validation screen. Although the effects of some pairs are inevitably missed due to the presence of additional drugs in the initial pool assay that interfere with synergistic effects, and the inherent variability of large scale screens, this method seems to be robust based on a separate validation screen, and has an estimated discovery rate of 46.7%. In addition to the detection of drugs with previously known activity against HIV, we identified several previously unknown anti-HIV reagents that warrant further investigation. This is especially true for the pairs that have effects in the late viral life cycle part of the part two assay of the screen. In addition, we demonstrate a significant enrichment of anti-inflammatory drugs in the anti-HIV synergistic drug network. Importantly, multiple studies have suggested that chronic inflammation is associated with

disease progression in AIDS patients<sup>24–29</sup>. Furthermore, clinical studies of AIDS patients on HAART therapies have revealed significant health problems caused by HIV-induced chronic inflammation<sup>30</sup>. While chronic inflammation contributes to infection-associated pathology, our results suggest that HIV propagation may be dependent on inflammation given the significant enrichment of anti-inflammatory agents in our screen. Importantly, studies in primates support the notion that suppression of immune activation may be a major protection mechanism that prevents disease progression in the natural hosts of simian immunodeficiency virus (SIV)<sup>31</sup>. Thus, anti-inflammatory therapies for AIDS should be investigated not only for relief of virus-associated pathology, but also to inhibit virus propagation. The *MuSIC* screening methodology not only identifies efficacious drug pairs, but also provides biological insight by producing drug-drug interaction networks. We envision that *MuSIC* could be used for a wide variety of disease-relevant screens, thereby allowing the efficient repositioning of drugs and drug pairs that can be rapidly moved into the clinic.

## Supplementary Material

Refer to Web version on PubMed Central for supplementary material.

## Acknowledgements

We thank the Institute of Chemistry and Cell Biology (ICCB)-Longwood: C. Shamu, S. Chiang, S. Rudnicki, A. Daab, D. Flood, S. Johnston, Z. Cooper, T. Ren; We also thank A. Engelman for help with virology, M. Mankowski for help with ELISA, M. Mefford for the BlaM assay protocol, J. Zhu, Q. Xu and other Elledge lab members for discussion, D. Fusco for reading the manuscript. X.T. is supported by the Damon Runyon Cancer Research Foundation (DRG 2008–09). Z.J.L. is supported by grants from the National Natural Science Foundation of China (31100601) and the National Key Basic Research Program (2012CB316503); S.J.E. is an investigator with the Howard Hughes Medical Institute.

## References and Notes

1. Lucas GM, Chaisson RE, Moore RD. Highly active antiretroviral therapy in a large urban clinic: risk factors for virologic failure and adverse drug reactions. *Annals of internal medicine*. 1999; 131:81–87. [PubMed: 10419445]
2. Hawkins T. Understanding and managing the adverse effects of antiretroviral therapy. *Antiviral research*. 2010; 85:201–209. [PubMed: 19857521]
3. Richman DD, et al. The challenge of finding a cure for HIV infection. *Science*. 2009; 323:1304–1307. [PubMed: 19265012]
4. Abdool Karim Q, et al. Effectiveness and safety of tenofovir gel, an antiretroviral microbicide, for the prevention of HIV infection in women. *Science*. 2010; 329:1168–1174. [PubMed: 20643915]
5. Jia J, et al. Mechanisms of drug combinations: interaction and network perspectives. *Nature reviews. Drug discovery*. 2009; 8:111–128.
6. Fitzgerald JB, Schoeberl B, Nielsen UB, Sorger PK. Systems biology and combination therapy in the quest for clinical efficacy. *Nature chemical biology*. 2006; 2:458–466. [PubMed: 16921358]
7. Borisy AA, et al. Systematic discovery of multicomponent therapeutics. *Proceedings of the National Academy of Sciences of the United States of America*. 2003; 100:7977–7982. [PubMed: 12799470]
8. Lehar J, et al. Synergistic drug combinations tend to improve therapeutically relevant selectivity. *Nature biotechnology*. 2009; 27:659–666.
9. Wilson-Lingardo L, et al. Deconvolution of combinatorial libraries for drug discovery: experimental comparison of pooling strategies. *Journal of medicinal chemistry*. 1996; 39:2720–2726. [PubMed: 8709102]

10. Severyn B, et al. Parsimonious discovery of synergistic drug combinations. *ACS chemical biology*. 2011; 6:1391–1398. [PubMed: 21974780]
11. Kimpton J, Emerman M. Detection of replication-competent and pseudotyped human immunodeficiency virus with a sensitive cell line on the basis of activation of an integrated beta-galactosidase gene. *Journal of virology*. 1992; 66:2232–2239. [PubMed: 1548759]
12. Brass AL, et al. Identification of host proteins required for HIV infection through a functional genomic screen. *Science*. 2008; 319:921–926. [PubMed: 18187620]
13. Hanley TM, Viglianti GA. Nuclear receptor signaling inhibits HIV-1 replication in macrophages through multiple trans-repression mechanisms. *Journal of virology*. 2011; 85:10834–10850. [PubMed: 21849441]
14. Russo FO, Patel PC, Ventura AM, Pereira CA. HIV-1 long terminal repeat modulation by glucocorticoids in monocytic and lymphocytic cell lines. *Virus research*. 1999; 64:87–94. [PubMed: 10500286]
15. Andrieu JM, Lu W. Long-term clinical, immunologic and virologic impact of glucocorticoids on the chronic phase of HIV infection. *BMC medicine*. 2004; 2:17. [PubMed: 15128452]
16. Ulmer A, Muller M, Bertisch-Mollenhoff B, Frietsch B. Low dose prednisolone reduces CD4+ T cell loss in therapy-naive HIV-patients without antiretroviral therapy. *European journal of medical research*. 2005; 10:105–109. [PubMed: 15851376]
17. Korba BE, et al. Nitazoxanide, tizoxanide and other thiazolides are potent inhibitors of hepatitis B virus and hepatitis C virus replication. *Antiviral research*. 2008; 77:56–63. [PubMed: 17888524]
18. Rossignol JF, La Frazia S, Chiappa L, Ciucci A, Santoro MG. Thiazolides, a new class of anti-influenza molecules targeting viral hemagglutinin at the post-translational level. *The Journal of biological chemistry*. 2009; 284:29798–29808. [PubMed: 19638339]
19. Bliss CI. The calculation of microbial assays. *Bacteriological reviews*. 1956; 20:243–258. [PubMed: 13403845]
20. Chou TC. Theoretical basis, experimental design, and computerized simulation of synergism and antagonism in drug combination studies. *Pharmacological reviews*. 2006; 58:621–681. [PubMed: 16968952]
21. Yeh P, Tschumi AI, Kishony R. Functional classification of drugs by properties of their pairwise interactions. *Nature genetics*. 2006; 38:489–494. [PubMed: 16550172]
22. Cavois M, De Noronha C, Greene WC. A sensitive and specific enzyme-based assay detecting HIV-1 virion fusion in primary T lymphocytes. *Nature biotechnology*. 2002; 20:1151–1154.
23. Collins SR, Schuldiner M, Krogan NJ, Weissman JS. A strategy for extracting and analyzing large-scale quantitative epistatic interaction data. *Genome biology*. 2006; 7:R63. [PubMed: 16859555]
24. Hazenberg MD, et al. Persistent immune activation in HIV-1 infection is associated with progression to AIDS. *AIDS*. 2003; 17:1881–1888. [PubMed: 12960820]
25. Deeks SG, et al. Immune activation set point during early HIV infection predicts subsequent CD4+ T-cell changes independent of viral load. *Blood*. 2004; 104:942–947. [PubMed: 15117761]
26. Giorgi JV, et al. Predictive value of immunologic and virologic markers after long or short duration of HIV-1 infection. *J Acquir Immune Defic Syndr*. 2002; 29:346–355. [PubMed: 11917238]
27. Hunt PW, et al. Relationship between T cell activation and CD4+ T cell count in HIV-seropositive individuals with undetectable plasma HIV RNA levels in the absence of therapy. *The Journal of infectious diseases*. 2008; 197:126–133. [PubMed: 18171295]
28. Douek DC, Roederer M, Koup RA. Emerging concepts in the immunopathogenesis of AIDS. *Annual review of medicine*. 2009; 60:471–484.
29. Eggena MP, et al. T cell activation in HIV-seropositive Ugandans: differential associations with viral load, CD4+ T cell depletion, and coinfection. *The Journal of infectious diseases*. 2005; 191:694–701. [PubMed: 15688282]
30. Deeks SG. HIV infection, inflammation, immunosenescence, and aging. *Annual review of medicine*. 2011; 62:141–155.
31. Chahroudi A, Bosinger SE, Vanderford TH, Paiardini M, Silvestri G. Natural SIV hosts: showing AIDS the door. *Science*. 2012; 335:1188–1193. [PubMed: 22403383]

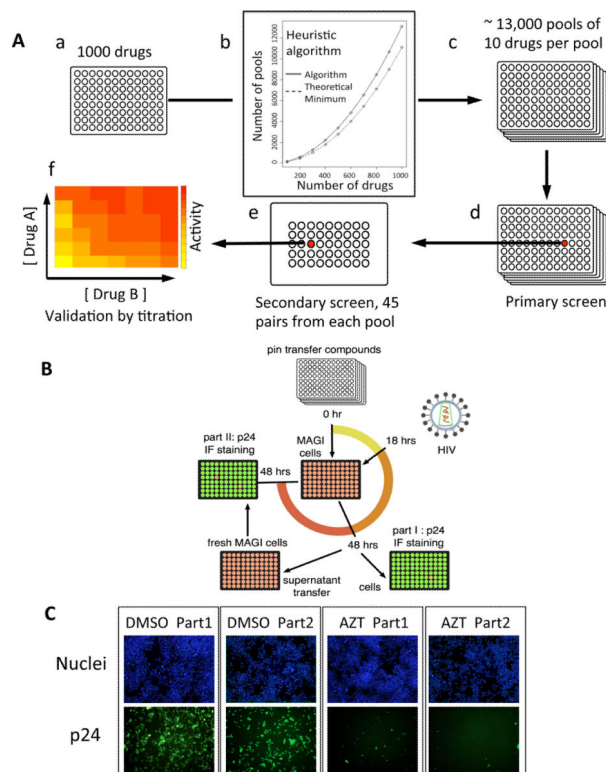


**Figure 1. *MuSIC* strategy and screening assay**

(A). Protocol of the *MuSIC* screen. a,b: 1000 drugs are constructed into a pooled library with 10 drugs per well using a heuristic algorithm to ensure that every pair-wise interaction is represented; c: primary screen using the pooled drug library; d: hits from primary screen are deconvoluted into pairs to construct the secondary library; e: deconvolution screen of the secondary library screen; f: hits from secondary library are validated using concentration titrations of the two drugs. (B) The screen assay protocol: for the part one assay, cells are plated on 384-well plates overnight before drug treatment. HIV is added to the cells 18 hours after drug treatment to allow the drugs to take effect (MOI = ~0.5). Forty-eight hours after adding virus, the cells are immunostained for HIV p24 expression and imaged to quantify the percentage of cells with positive staining, indicating the infection rate. The supernatant from the part one assay is transferred to new plates with fresh cells to initiate the part two assay for quantification of newly generated virus. Forty-eight hours later, the part two plates are also stained and imaged. (C) Part one and part two staining images of positive control (1 $\mu$ g/ml AZT) and negative control (DMSO) used in the screen. Top row: DAPI staining of cell nuclei for the quantitation of cell number and monitoring cytotoxicity. Bottom row: p24 staining of HIV infected cells.

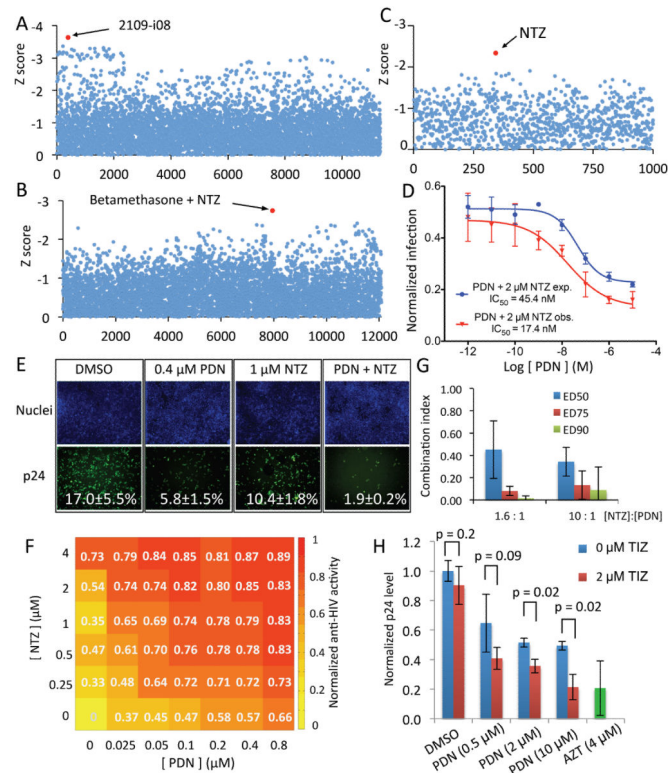


**Figure 2. *MuSIC* screen identified synergistic drug combinations**

(A) Distribution of Z scores for infection rates in the primary screen, showing drug pools that have anti-viral activity in the part one assay ( $Z$  score  $< 0$ ), the  $x$  axis indicates the drug pools. The pool highlighted in red contains betamethasone and nitazoxanide (NTZ). (B) The distribution of Z-scores for infection rates in the secondary screen illustrating drug pairs that have anti-viral activity in the part two assay ( $Z$  score  $< 0$ ). The  $x$ -axis indicates the drug pair. (C) The distribution of Z-scores for infection rates in the glucocorticoid synergizer screen illustrating drugs that have additional anti-viral activity when combined with the glucocorticoid prednisolone (PDN). NTZ (highlighted in red) was identified as the top compound. (D) Dose response curves for the glucocorticoid, PDN in combination with  $2 \mu\text{M}$  NTZ. Blue: expected dose response curve based on the assumption that PDN and NTZ work independently and calculated with individual drugs' effects. Red: the observed response curve for PDN and NTZ demonstrates a synergistic effect. Infection rates are normalized to DMSO treated experiment. (E) Immunostaining images of the validation experiment showing the synergistic anti-HIV activity between PDN and NTZ. White numbers are the average infection rates and standard deviations of four replicate experiments. (F) Two-way titration experiment to calculate the Combination Index (CI). Inset values show normalized inhibition of HIV infection rate in the part two assay. (G) Combination Indices (CI) of the NTZ-PDN pair combination at EC50 (50% effective concentration), EC75 and EC90 calculated using the CalcuSyn program (1.6:1 and 10:1). Two mixing concentration ratios are used (1.6:1 and 10:1).  $\text{CI} < 1$  indicate synergy,  $\text{CI} < 0.3$  indicates strong synergy,  $\text{CI} < 0.1$  indicates very strong synergy<sup>20</sup>. (H) Validation of the PDN-tizoxanide pair in PBMCs using an ELISA for p24. Data is representative of PBMCs from three different donors. P-values were calculated using Student's t-test.

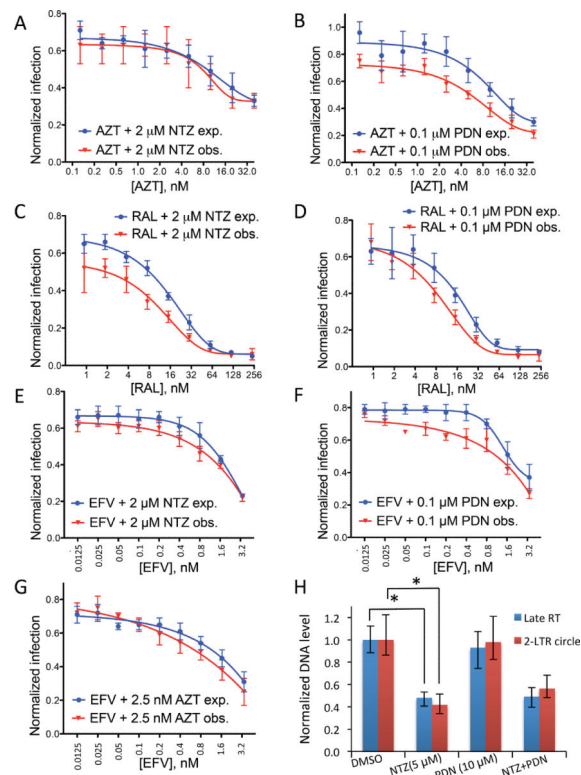


**Figure 3. Interactions with known anti-virals reveal drug mechanism**

(A, B): Dose response curves for the reverse transcriptase AZT in combination with 2  $\mu$ M NTZ or 0.1  $\mu$ M PDN showing synergy between PDN and AZT, but not between NTZ and AZT. Blue curve: expected curve based on the assumption that two drugs work independently and calculated with individual drugs' effects, red curve: observed curve of the combination. (C, D): Dose response curves for the integrase inhibitor raltegravir (RAL) in combination with 2  $\mu$ M NTZ or 0.1  $\mu$ M PDN showing that both PDN and NTZ synergize with RAL. (E, F, G): Dose response curves of the another reverse transcriptase inhibitor efavirenz (EFV) in combination with either 2  $\mu$ M NTZ, 0.1  $\mu$ M PDN or 2.5 nM AZT. In this case, only PDN shows significant synergy with EFV. (H) Q-RT-PCR quantitation of pseudotyped HIV NL43 reverse transcription products in MAGI cells: late RT and 2-LTR circle. Levels are normalized to mitochondria DNA, \* indicates P-value < 0.05 (Student's t-test).

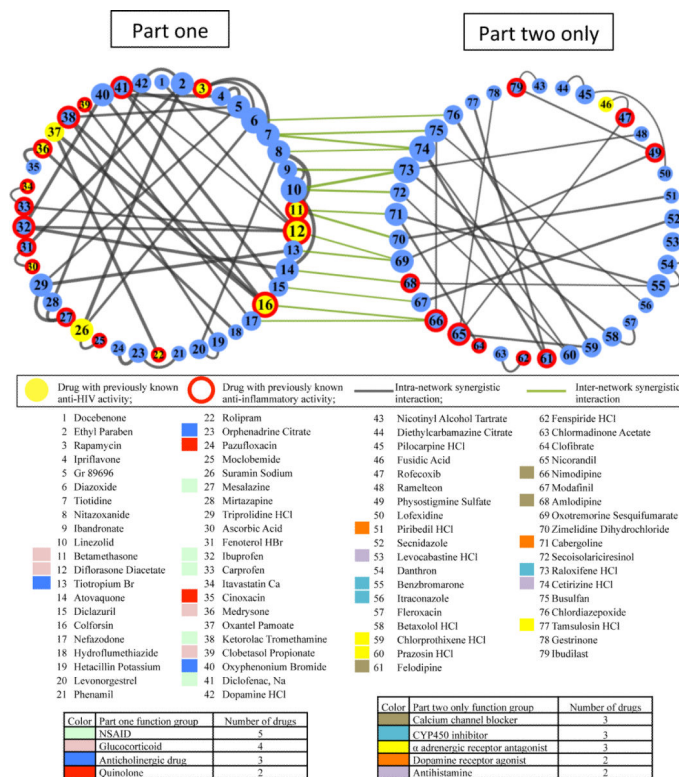


**Figure 4. Drug synergy network analysis reveals enrichments of drugs with known anti-HIV activity and anti-inflammatory functions**

The network of drug synergy shows drug pairs that have significant anti-viral activity and synergy (see supplemental text for the details on how the drugs were selected). Each drug is depicted by a circle with its size correlating with the number of drugs it has synergy with. Yellow circles indicates compounds with previously detected anti-HIV activity, red outer circles indicate known anti-inflammatory function. The part one network is highly enriched for drugs with previously detected anti-HIV activity ( $p < 10^{-12}$ ) and drugs with known anti-inflammatory activity ( $p < 10^{-4}$ ). The number in the circle is the index of the drug with the drug name shown in the list below. The line linking two drugs indicates synergy with the width of the line correlating with the strength of the synergy, the wider the line, the stronger the synergy. The green lines linking the two networks represent synergistic interactions between the two networks. The color blocks designate the functional groups that have more than one drug represented in each network. The names of the functional groups and the number of drugs belonging to each functional group are shown in the two tables below.